OSU Interim Project Report

1 Executive Summary

The research effort of the Ohio State University team led by Dr. Chi-Chih Chen has been focusing on (1) collecting VRU doppler responses using a commercial grade automobile radar in controlled environments, (2) identifying micro-doppler (MD) signatures which are unique to VRUs, and (3) developing VRU MD signatures extraction algorithms.

So far, we have been collected and analyzed MD data collected from different pedestrian scenarios including different combinations of arm and leg movements as well as different walking speeds and directions. Some measurement data and MD processed results will be presented in Section 4.1.

A robust statistical-based MD extraction algorithms were subsequently developed and tested using these data. We have found that standard deviation of target velocity profile over a short duration of time provides a robust way of identifying the swing speed of arms and legs uniquely associated with pedestrians, and applying FFT over time at different velocity bin can capture their swing frequency. The details of this extraction methodology will be discussed in Section 3.

To help understanding the micro-doppler responses of swinging arms and legs collected by the automobile radar as a function of time, we performed measurement on rotating metal balls. By varying the number of balls and rotating speeds, we were able to verify the accuracy of the developed MD extraction algorithms. Samples of these data and processed results will be discussed in Section 3.

We also compared these featured obtained from radar measurement data and from high-speed camera captured human walking data available at OSU MoCap lab[1]. Both datasets showed similar features. The combination of these two features (speed and frequency) should allow one to separate pedestrians from other on-road targets. We will continue studying and improving the algorithm/codes for extracting swing speed and frequency in more complex target environments, i.e. in the presence of other moving objects in the scene. More details about MD analysis of MoCap data will be discussed in Section 4.2

We also started the data collection of bicyclist MD signatures, beginning with a single spinning wheel without rider. All other moving parts such as both wheels, pedals, and rider will be subsequently added one by one.

All the collected radar range-velocity data have been archived and easily accessible and reprocessed using Matlab functions. A separate Excel spreadsheet which lists all measurements completed to date will also be attached.

[1] https://accad.osu.edu/research/motion-lab/mocap-system-and-data

2 VRU Radar Micro-Doppler Feature Extraction Algorithms

Figure 2 shows the novel VRU micro-Doppler (MD) feature extraction algorithm developed by the OSU team based on measured data of difference pedestrian motions and rotating metal balls. The top left plot shows an example standard radar output frame in a 2D range-velocity format for a pedestrian jogging towards radar. The detected RCS level is indicated by the grey scale. The output frame rate depends on the radar. For the SmartMicro's DRIVEGRD 152 radar that we are using, the frame rate is 0.15 s/frame. Notice the presence of micro-doppler response is indicated by the presence of a horizontal spreading at the target position, signifying the presence of moving parts on the target.

The top right plot shows the collected tracked target velocity response different measurement time. The solid bright band observed around 3 m/s velocity bin correspond to the target's jogging speed. The bright yellow color is due to stronger scattering intensity from the torso. The vertical velocity spreading is produced by scattering from the arms and legs whose speeds with respect to radar a slightly different from that of the torso. The seemly random spreading is due to multiple moving parts, namely 2 arms and 2 legs, and the under-sampling effects associated the radar's slow frame rates relative to the motion speeds. If there is only a single arm moving at a higher frame rate, this image will appear more like a sinusoidal pattern as illustrated from high-speed camera motion captured data shown in Figure 14. This is a very important finding and motivated us to adopt statistical approach for analyze and extracting MD signatures.

The middle right "velocity detection binary plot" is the first step in our MD feature extraction. This binary plot is derived from the top right plot by applying thresholding. If the target response at a (time, velocity) pixel is greater than a pre-selected detection threshold, then the value at that pixel is set to 1. Otherwise, it is set to zero. Currently, the STD of the entire top right map is used as the threshold.

From the velocity detection plot, the standard deviation of detection over time at each velocity bin is calculated, which produce the middle left "velocity STD plot". There are three features contained in this velocity plot: (1) MD velocity range that shows maximum and minimum MD velocity, (2) symmetry of MD velocity, and (3) shape of MD velocity profile. For instance, the example shown here shows asymmetric MD and one side stop at zero velocity due to the moments when feet are in contact with ground. Also, the profile is not uniform and tilted towards low velocity region, which is associated with the longer durations at both ends the arms' and legs' swing motion. It would have been more uniform, i.e. flat top in the case of continuous rotation, as will be shown in Section 3 for rotating balls cases.

From the velocity detection map (middle right), we can also calculate velocity probability at each measurement time by taking the velocity weight mean, i.e. (velocity)*(pixel value)/(total number of pixels), which generates the green dashed line in the bottom right picture. To remove the velocity bias, the mean velocity (blue line) is subtracted out to obtain the unbiased red line. As seen, there is some kind of oscillatory behavior in the waveform which should be associated with

the repetitive swinging motions of arms and legs. To retrieve the oscillation frequency, we apply FFT to the red lines and the resultant frequency spectrum is plotted in the bottom left picture which reveals a clear pick around 2.585 Hz. This is the fourth VRU MD feature extracted from radar data.

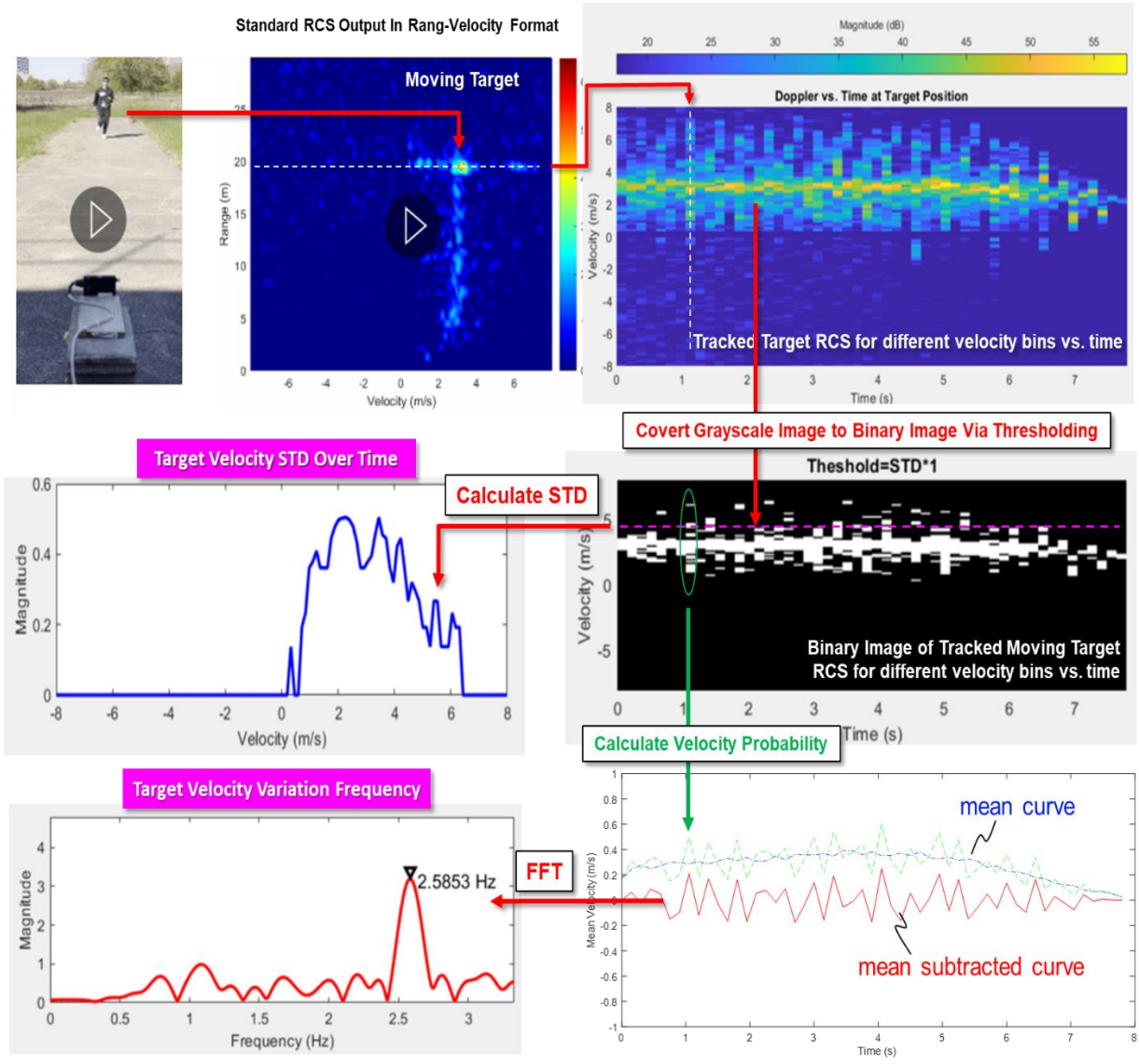

Figure 1 – OSU VRU micro-Doppler (MD) feature extraction algorithm.

3 Micro-Doppler Radar Data Collection of Rotating Spheres

To help understanding the meanings and accuracy of the extracted MD features discussed in the previous section, we conducted similar radar measurements and MD data processing for rotating metal balls using the setup shown in Figure 2. Each ball is made of 6" diameter Styrofoam sphere that is covered with kitchen aluminum foils. These balls were attached to the end of a 2 feel long rod whose center was attached to an electrical drill used turning the balls manually. The number

of balls was varied from 1 to 4. Three different rotating speeds: slow, medium, and fast were performance for each case.

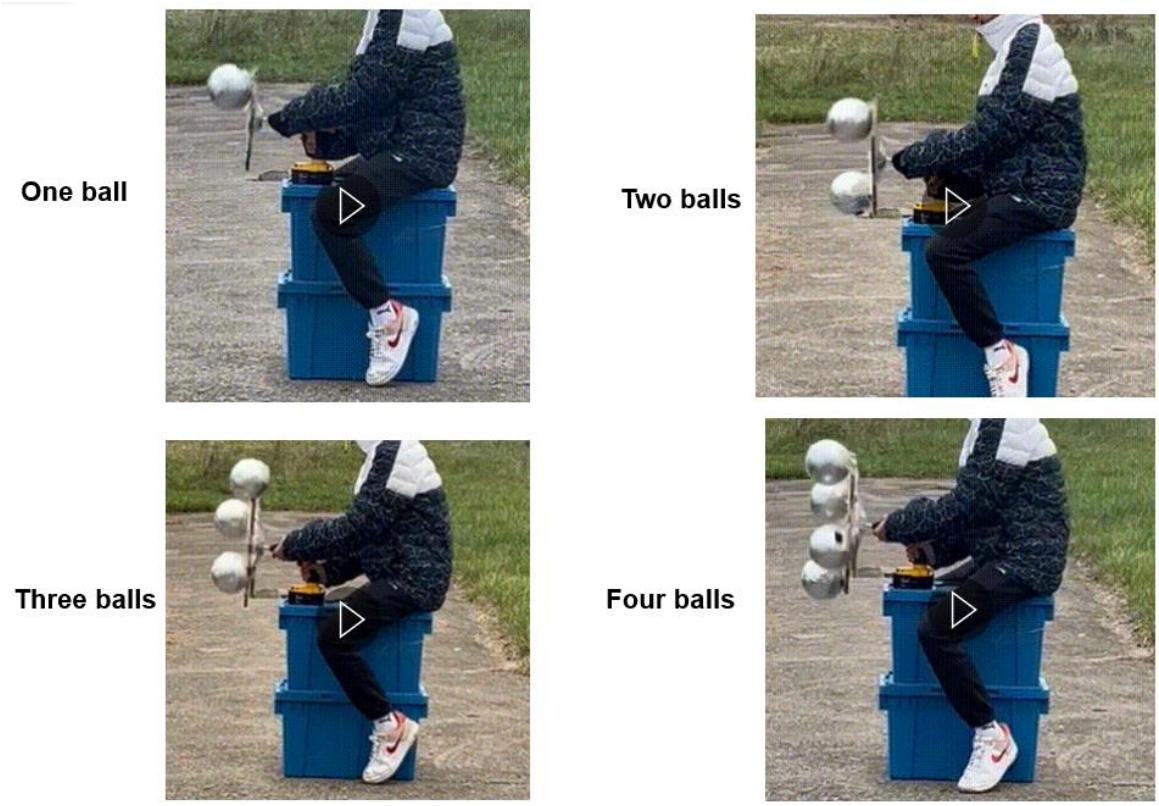

Figure 2 – Test setup for studying the micro-doppler response of rotating metal balls.

The top plot in Figure 3 shows measured tracked target velocity response for a single ball rotating a slow speed. The velocity STD plot shows the maxim speeds of ball moving towards and away from the radar at 1.6 m/s and 2.1 m/s, respectively. The profile of the velocity STD plot is relative flat at the top, which is different from what observed in the pedestrian case in Figure 1. The velocity frequency analysis at the bottom plot shows a clear oscillation/rotation frequency around 1.42 Hz which should correspond to 1/1.42 seconds per revolution.

Similarly, Figure 4 shows another example of measured and processed data for a single fast-rotating metal ball. The frequency analysis at the bottom now shows a higher frequency of approximately 3.05 Hz. The velocity STD plot also shows a wider velocity range up to approximately 4.5 m/s compared to Figure 3. The last example in Figure 5 shows the results for three slowly rotating balls. Notice the relatively flat top behavior in all three velocity STD plots. These rotating sphere test results further demonstrate that the developed MD analysis tools seems to be able to extract the radar MD signatures accurately and effectively.

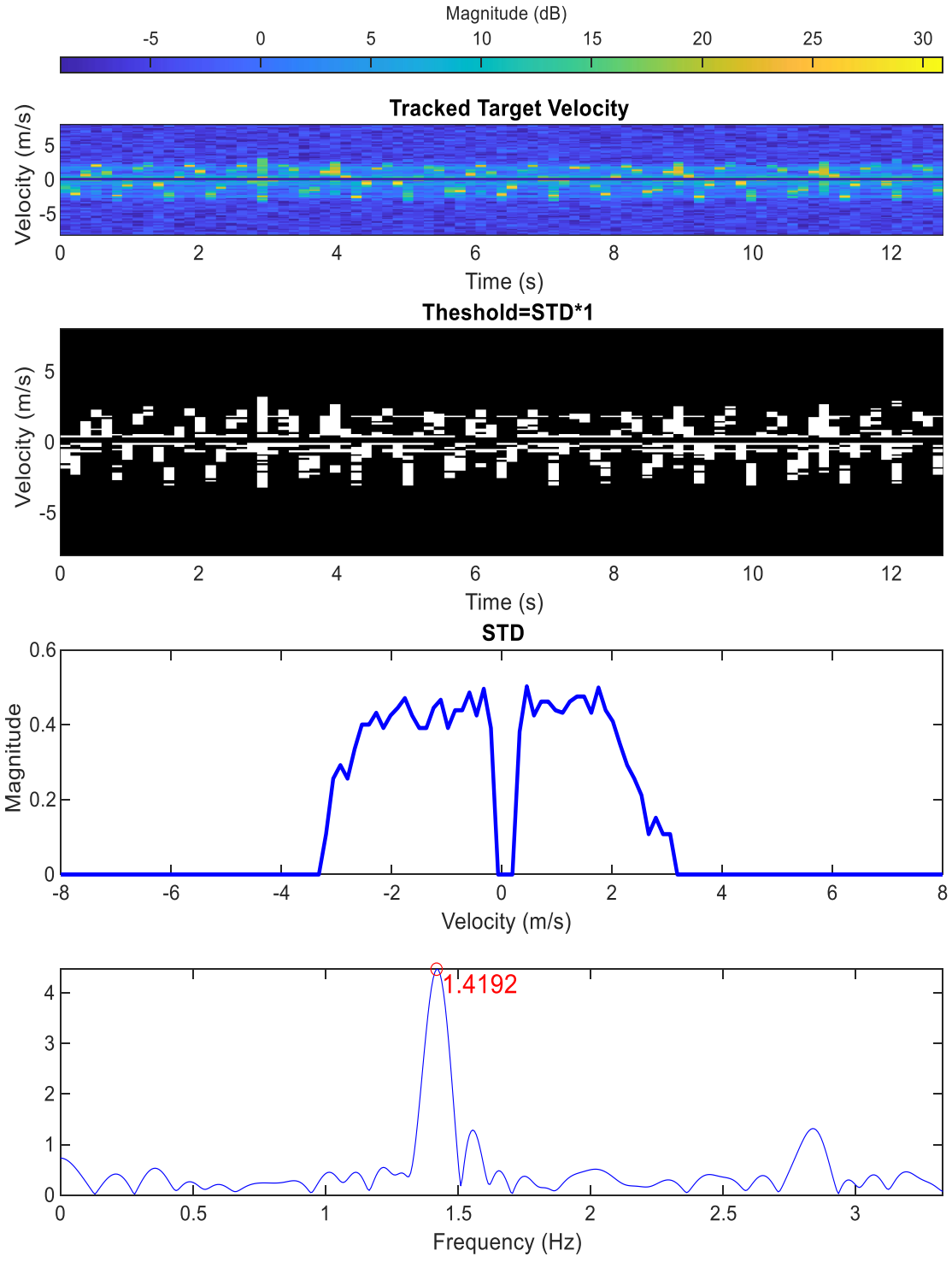

Figure 3 – Measured target velocity data (top row) and its processed MD results for a single slowly rotating ball.

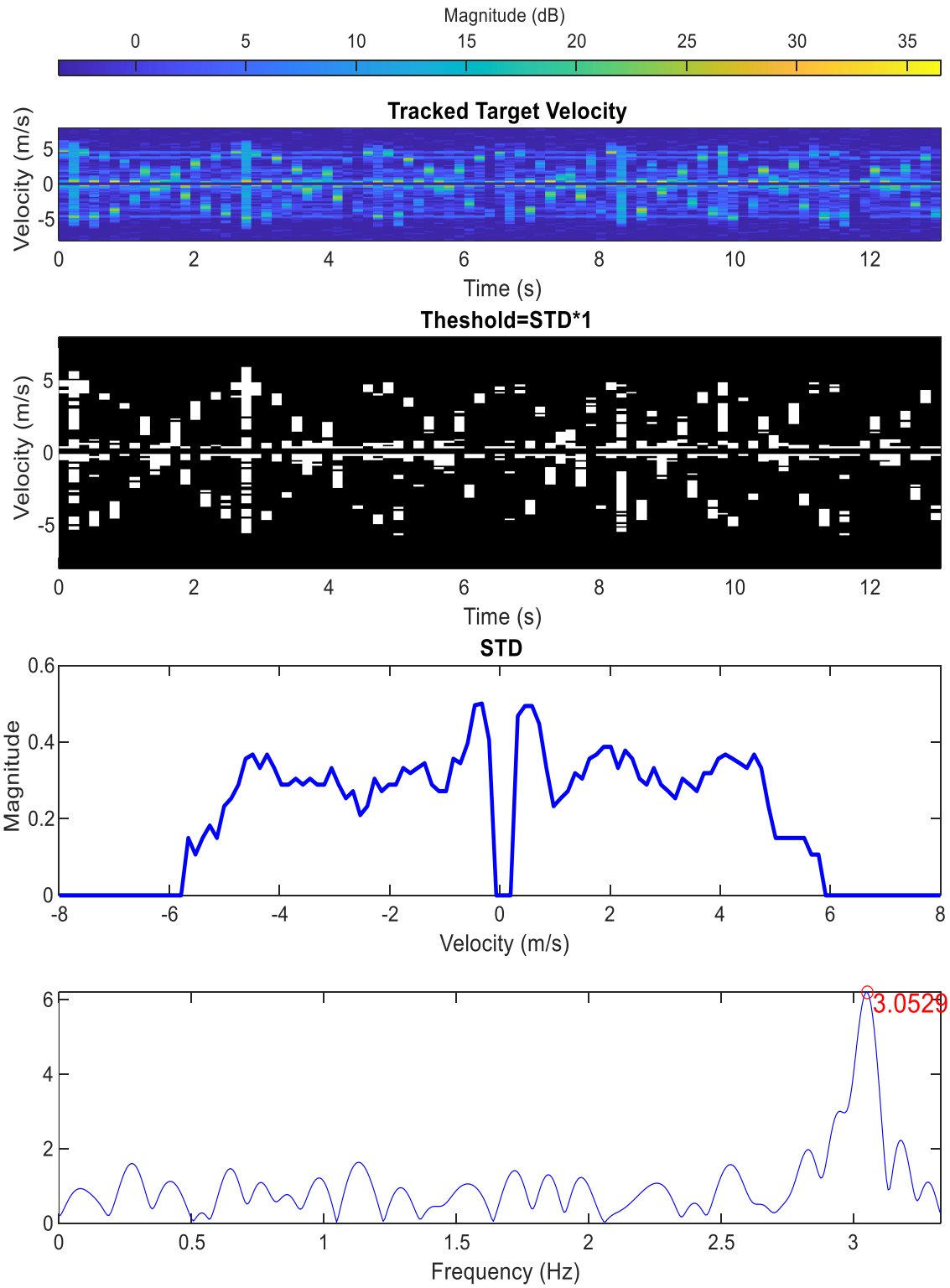

Figure 4 - Measured target velocity data (top row) and its processed MD results for a single fast rotating ball.

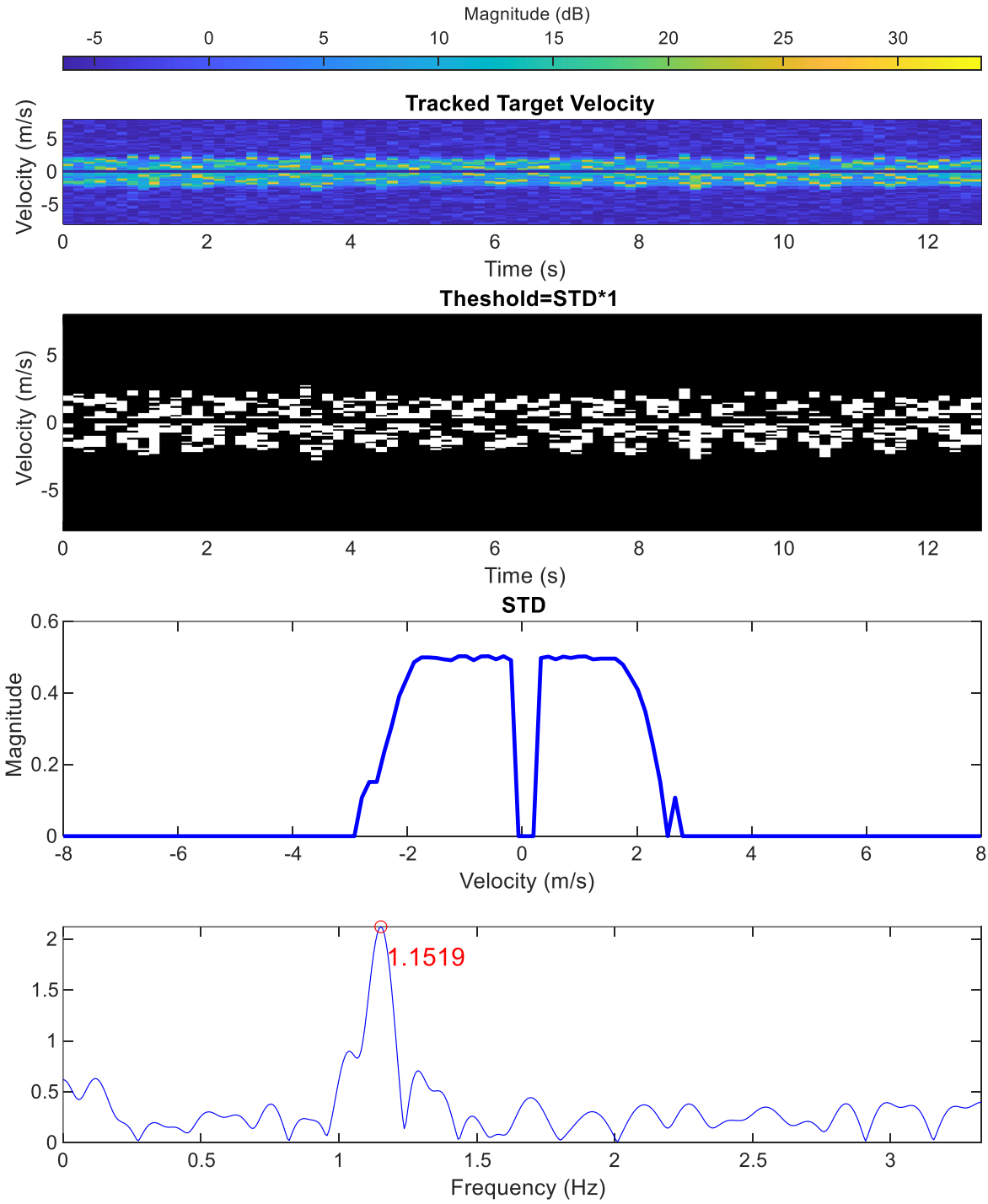

Figure 5 - Measured target velocity data (top row) and its processed MD results for three slowly rotating balls.

4 Pedestrian Micro-Doppler Study

4.1 Micro-Doppler Radar Data Collection of Pedestrians

The radar data of various pedestrian motion configurations for studying pedestrian micro-doppler signatures have been collected on OSU-ESL's outdoor concrete pad side. Measurements were conducted with the radar positioned approximately 0.5 meters above the ground and targeting distances ranging from 5 to 25 meters, as seen in Figure 6. We have collected data with pedestrian moving at three different speeds (normal walking, fast walking, and jogging) and in different directions (towards radar, away from radar, and crossing radar beam). We also included different combinations of arm and leg motions: no moving arms and legs, moving arms only, moving legs only, moving both arms and legs. The data and processed results below serve as examples of some of these cases.

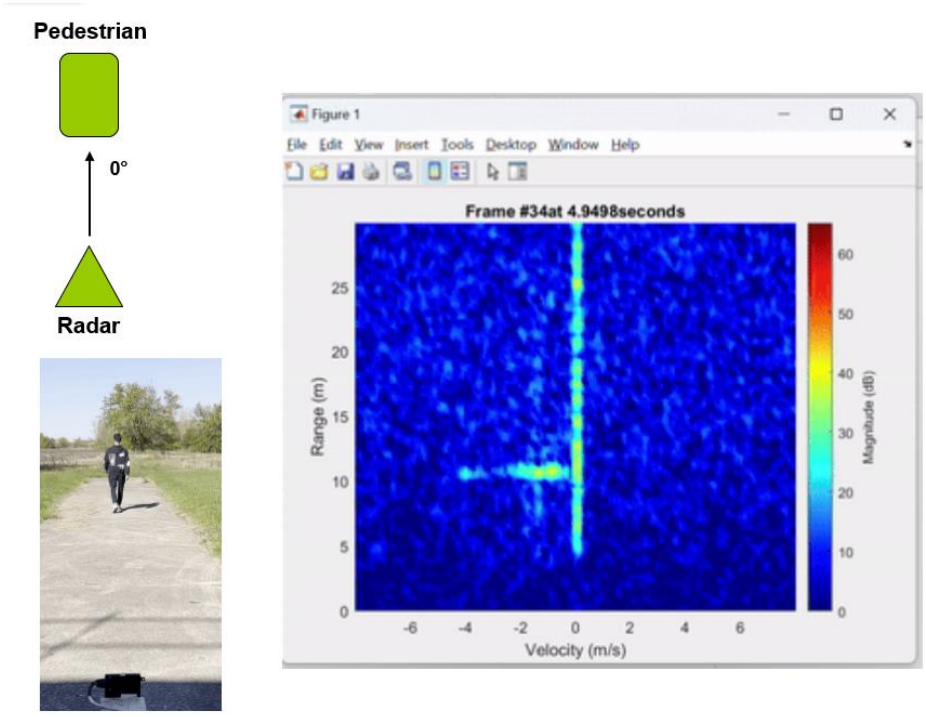

Figure 6 - Pedestrian micro-doppler data collection on OSU-ESL's concrete pad.

Using the developed MD processing algorithm explained in Section 2, each pedestrian motion case was processed to study the MD signatures associated with the motions of arms and Legs which are unique to pedestrians. Figure 1 shows the processed results of the first example where a pedestrian walked towards radar at a normal speed without moving arms so that we can isolate the MD response associated with legs movements. The MD velocity STD plot (third plot) shows the unique feature where velocity stays on one side of the sign and drops sharply at zero velocity. The MD velocity is positive when the target is approaching radar and is negative when the target is leaving radar. The sharp drop off occurs when the legs are on the ground. This will be further

discussed in Section 4.2. This is a very distinct MD velocity associated with “walking”. The MD frequency analysis shows three dominant peaks at 1.18 Hz, 1.84 Hz, and 3.00 Hz, where the lowest frequency of 1.18 Hz should be the swing frequency of the legs and arms. The other higher frequencies are likely associated with the harmonics since the motion of legs and arms are not exactly “on beats” and will have some variations in speed. This is certainly different from the nice MD frequency spectrum observed in the rotating sphere cases discussed in Section 3. Regardless, such spectrum behavior is practical and real and can be used as a part of VRU MD signatures to train future machine-learning detection algorithms.

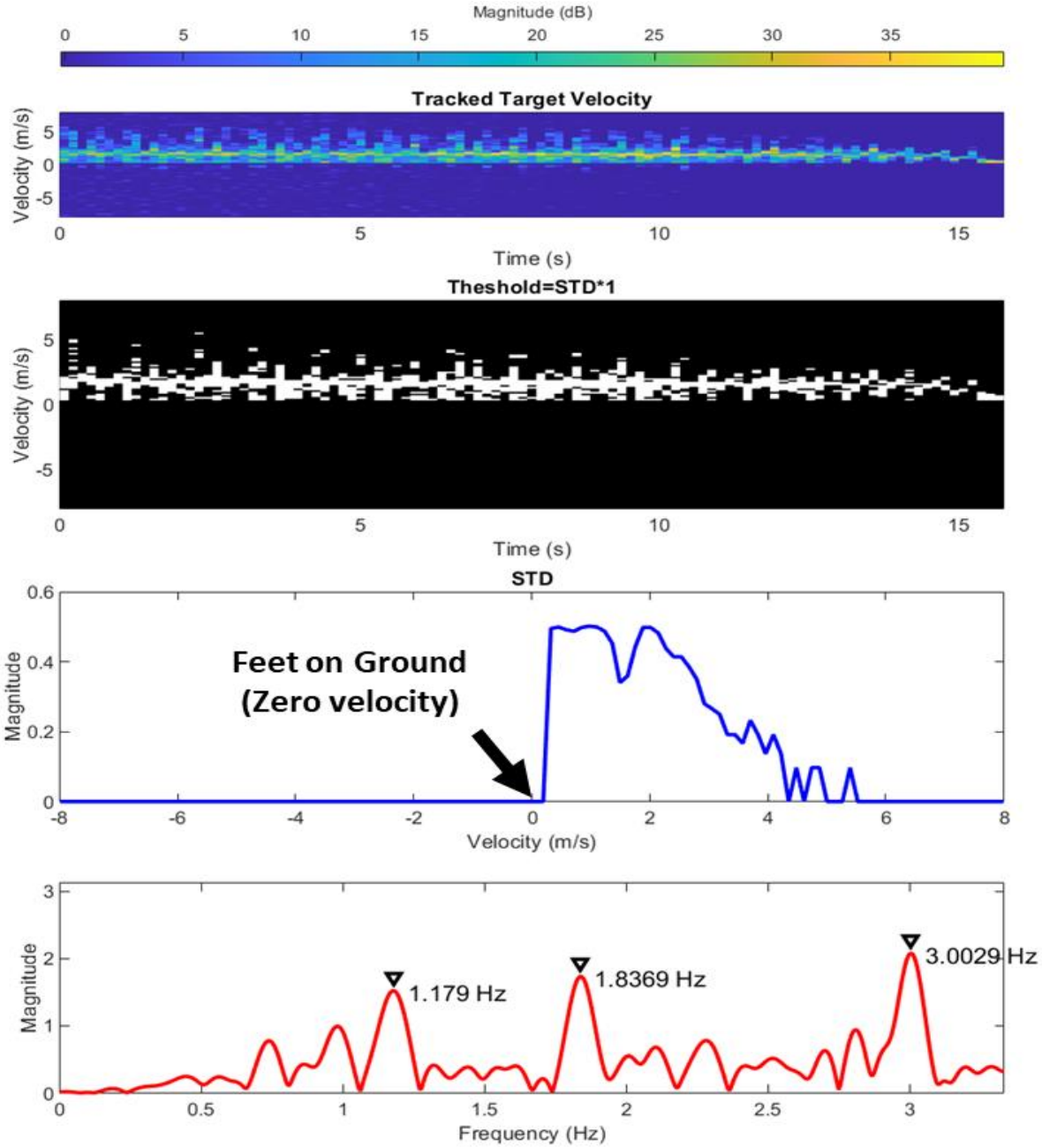

Figure 7 –Processed MD signatures of pedestrian walking towards radar without moving arms.

Figure 8 shows the tracked target velocity response and its MD processed results for a pedestrian walking towards radar normally with legs and arms moving. Compared the results for the fixed arm case in Figure 7, one can notice the appearance of some response in the negative velocity. This is produced by the scattering the arms that swing backwards beyond the body, and away from the radar. It should be noted that the notch around the zero velocity is due to a narrow band filter in the processing algorithm to suppress the zero doppler responses which are often associated with background scattering from the environments. The bottom MD frequency plot shows a similar frequency information as in the previous fixed arm case. This is expected since the movement of arms and legs should be synchronized most of the time.

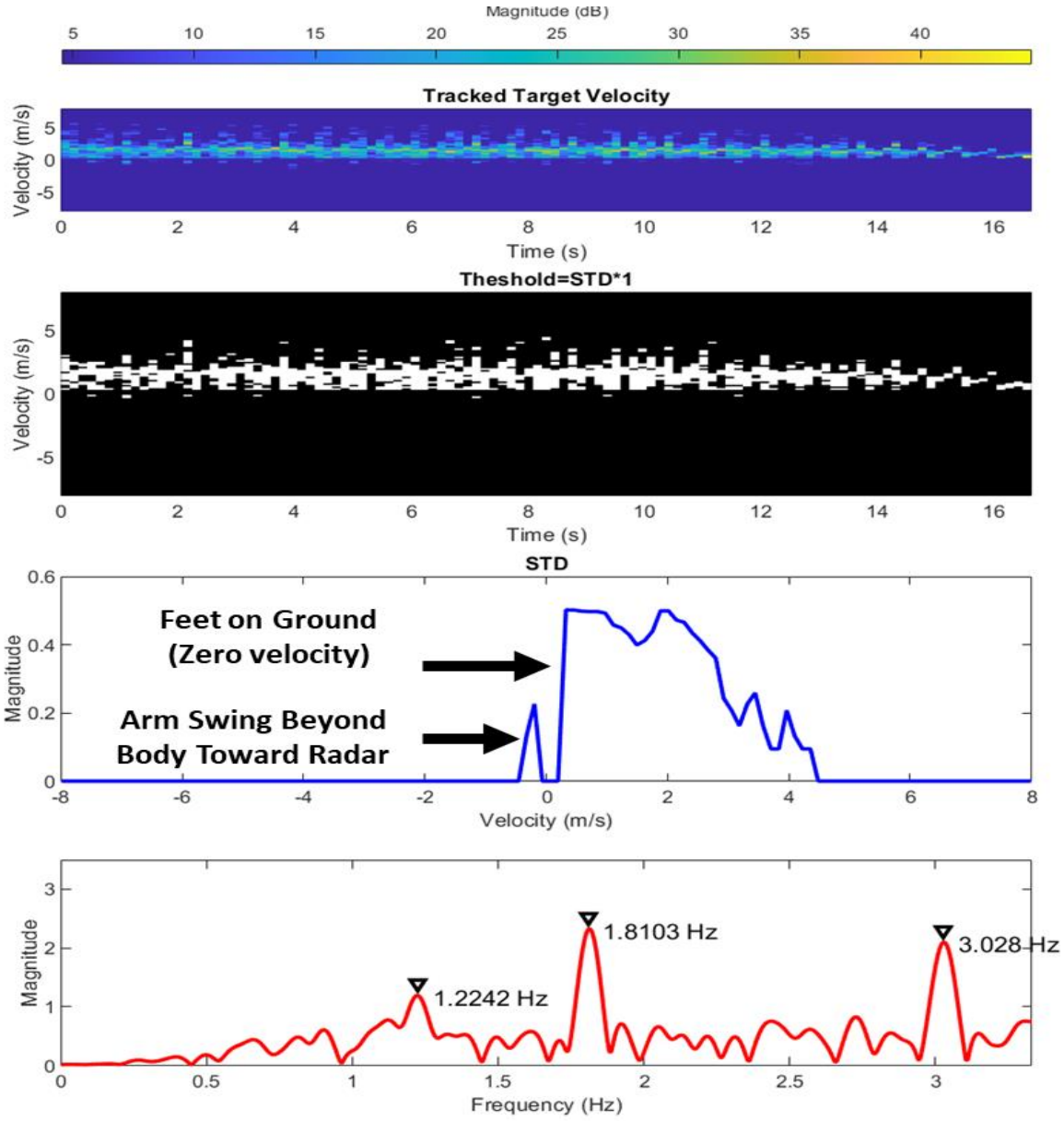

Figure 8 - Processed MD signatures of pedestrian normal walking towards.

Figure 9 shows the MD processed results for a pedestrian jogging toward radar. Compared to the previous walking case, the MD velocity STD pattern shifts to the higher speed direction (right side) as expected and stay in the positive velocity region. Notice that even the arms can swing behind the body, they are still moving towards radar because of momentum. The frequency analysis shows two prominent peaks at around 1.09 Hz and 2.59 Hz, where 1.09 Hz is likely the swinging frequency of arms and legs. This frequency is lower than walking because of the longer strides during jogging. Similarly, Figure 10 shows the MD processed results for a pedestrian jogging away from radar. The swing frequency of 1.11 Hz is more pronounced in this case.

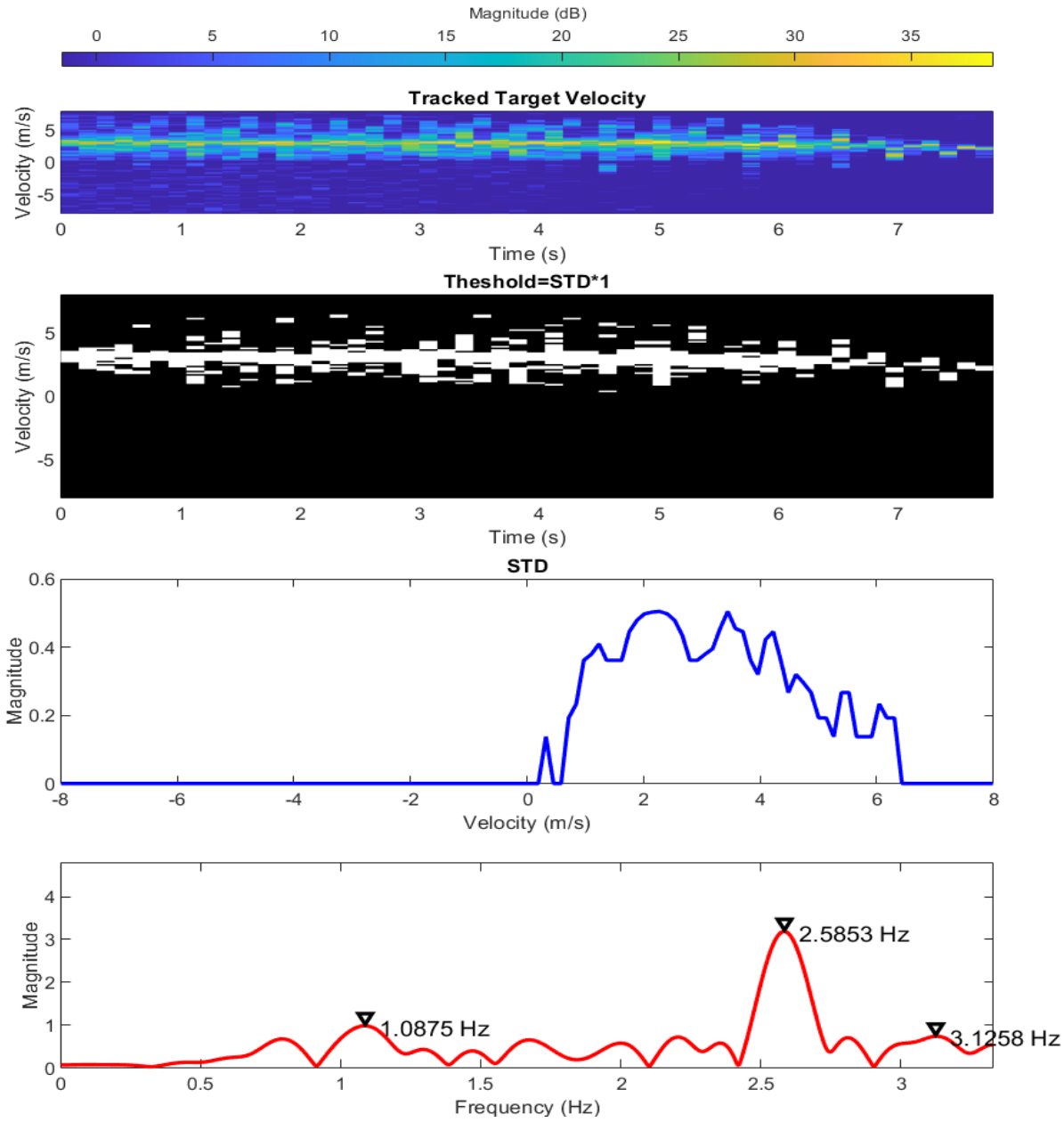

Figure 9 - Processed MD signatures of pedestrian jugging towards radar.

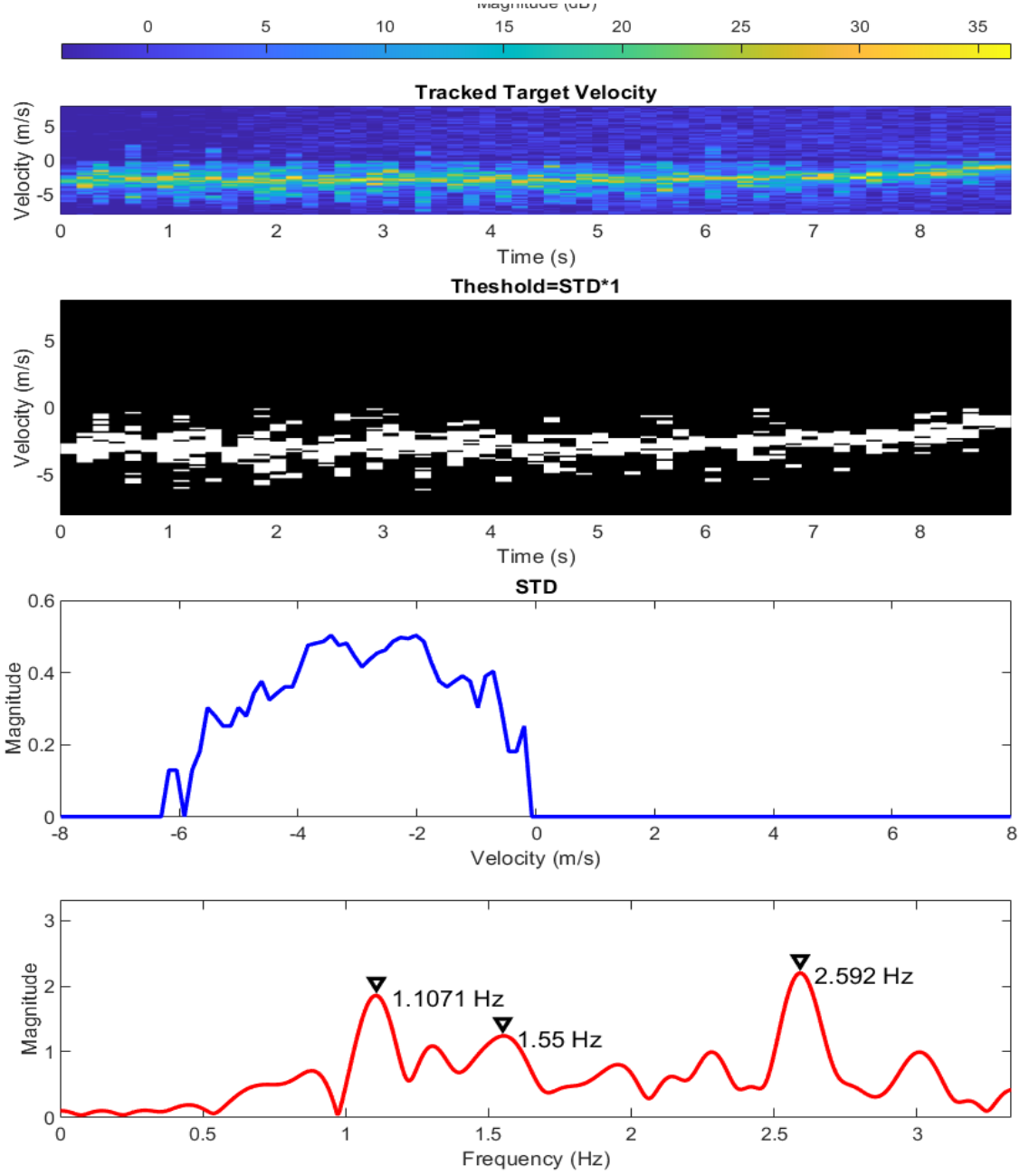

Figure 10 - Processed MD signatures of pedestrian jogging away from radar.

Figure 11 shows the MD processed results for a pedestrian waking across the radar beam at the distance of 10 meters from radar. It is interesting that the MD features are still quite detectable. The MD velocity STD plot show symmetric “cosine” like of pattern and the swing frequency of arms and legs are clearly detected at 0.96 Hz. Of course, it is expected that MD responses will become less detectable as crossing distance to radar increases. It should be pointed out the radar beam was digitally steered to track the target in our data processing.

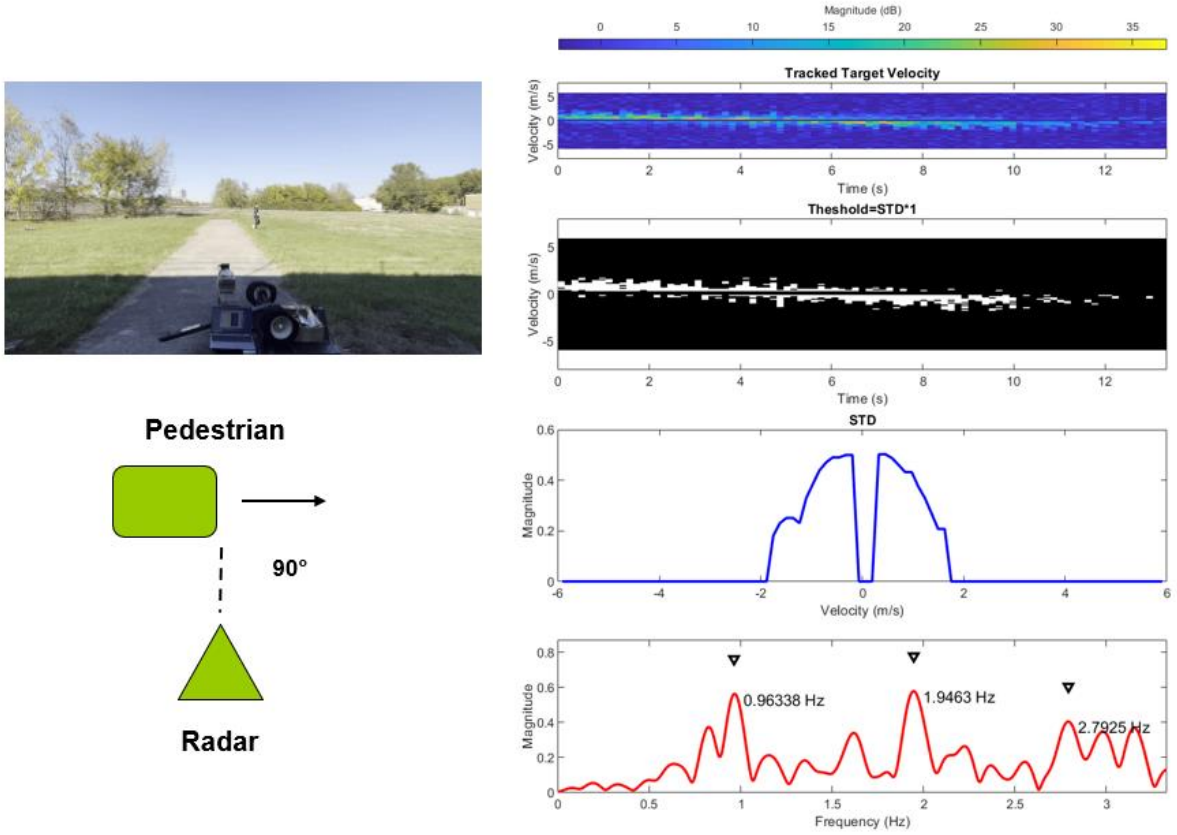

Figure 11 – Processed MD signatures of pedestrian walking across radar at 90 degrees.

4.2 Radar Micro-Doppler of Pedestrian Extracted from OSU High-Speed Camera Captured Motion (MoCap) Dataset

To help understanding the motion of arms and legs motions and their theoretical radar MD STD, we also studied the motion dataset captured by the OSU Advanced Computing center for Arts and Design's MoCap System using high speed cameras, as shown in Figure 12. We have selected a few motion captured files which include human walking and running in the MoCap dataset and isolated out the motion of joints on legs and legs to study their velocity properties. Figure 13 shows an example of the high-speed camera captured velocity profiles of joints on arms and feet during an actual human walking toward radar. These results confirm two MD features discussed in Section 4.1. The first feature is that the MD velocity of legs have hard stops at zero velocity when the feet land on ground. The second feature is that the MD velocity of arms will go beyond zero velocity during walking when arms swing back faster than walking speed. The bottom right plot Figure 14 shows Processed MD velocity STD data from actual motion captured data of arms and feet using our MD extraction algorithm. The bottom left plot is the binary velocity response data. This shows a much clearer sinusoidal oscillatory behavior compared to actual radar measured data because of (1) higher sampling rate and (2) angle-dependent radar scattering intensity of arms and legs.

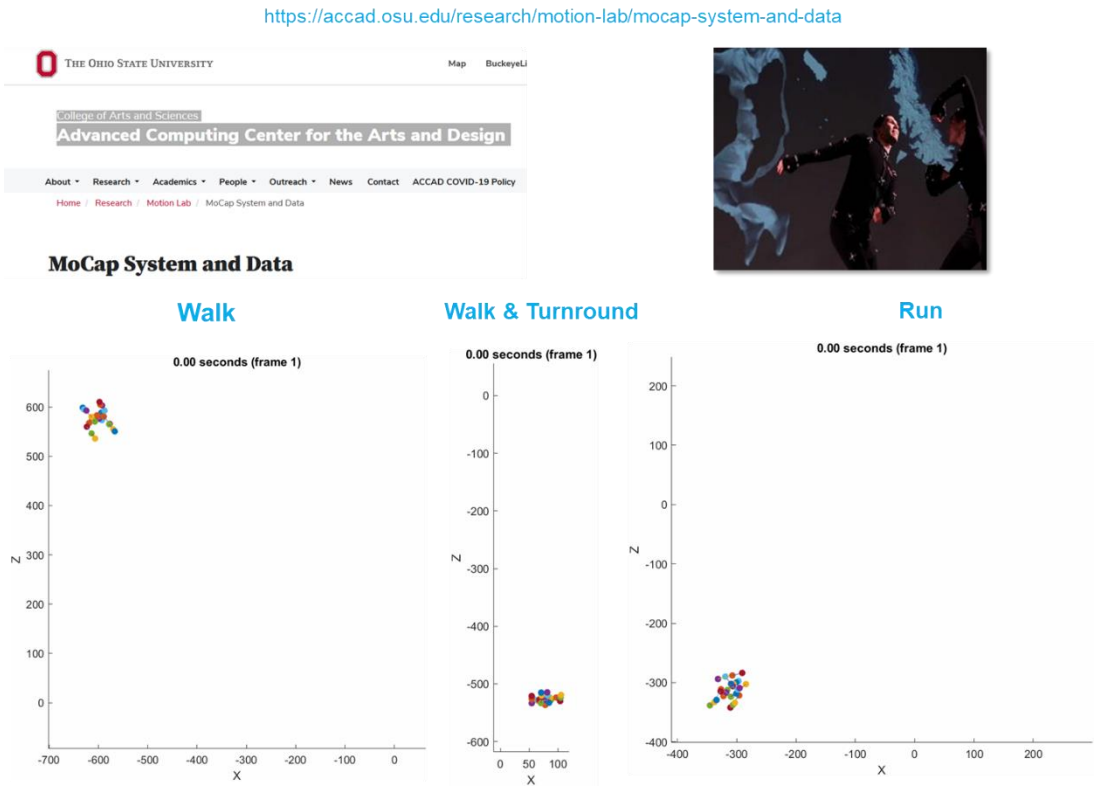

Figure 12 – OSU Advanced Computing center for Arts and Design's MoCap System.

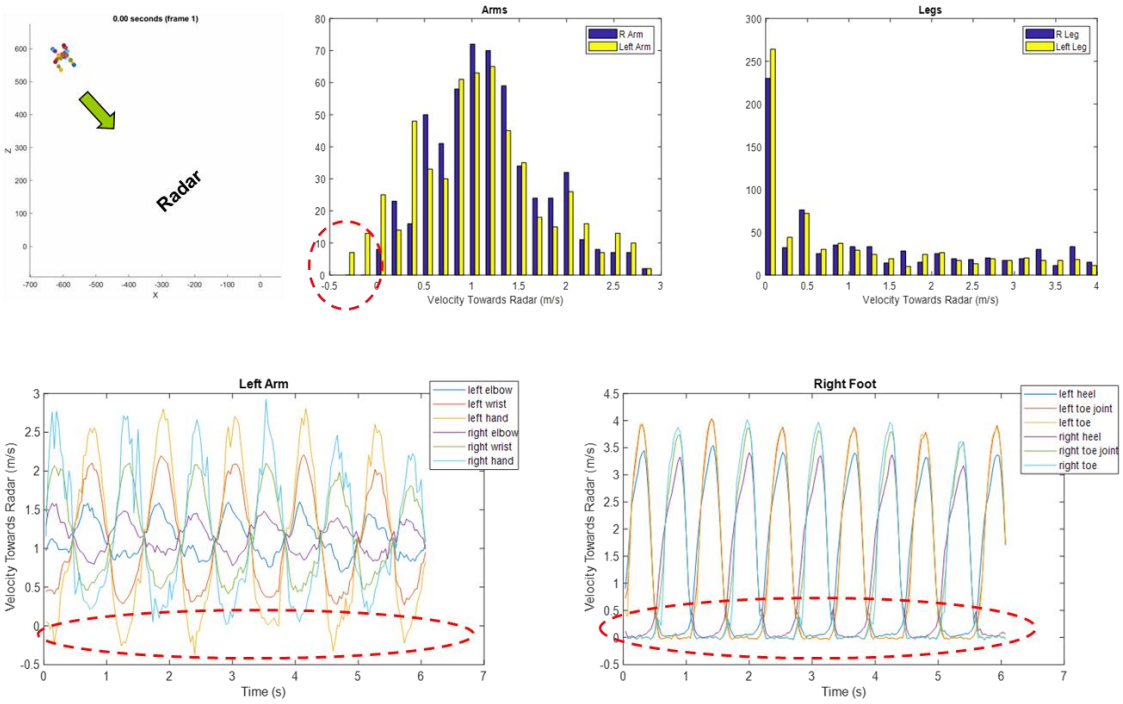

Figure 13 – The high-speed camera captured velocity profiles of joints on arms and feet during an actual human slow walking toward radar.

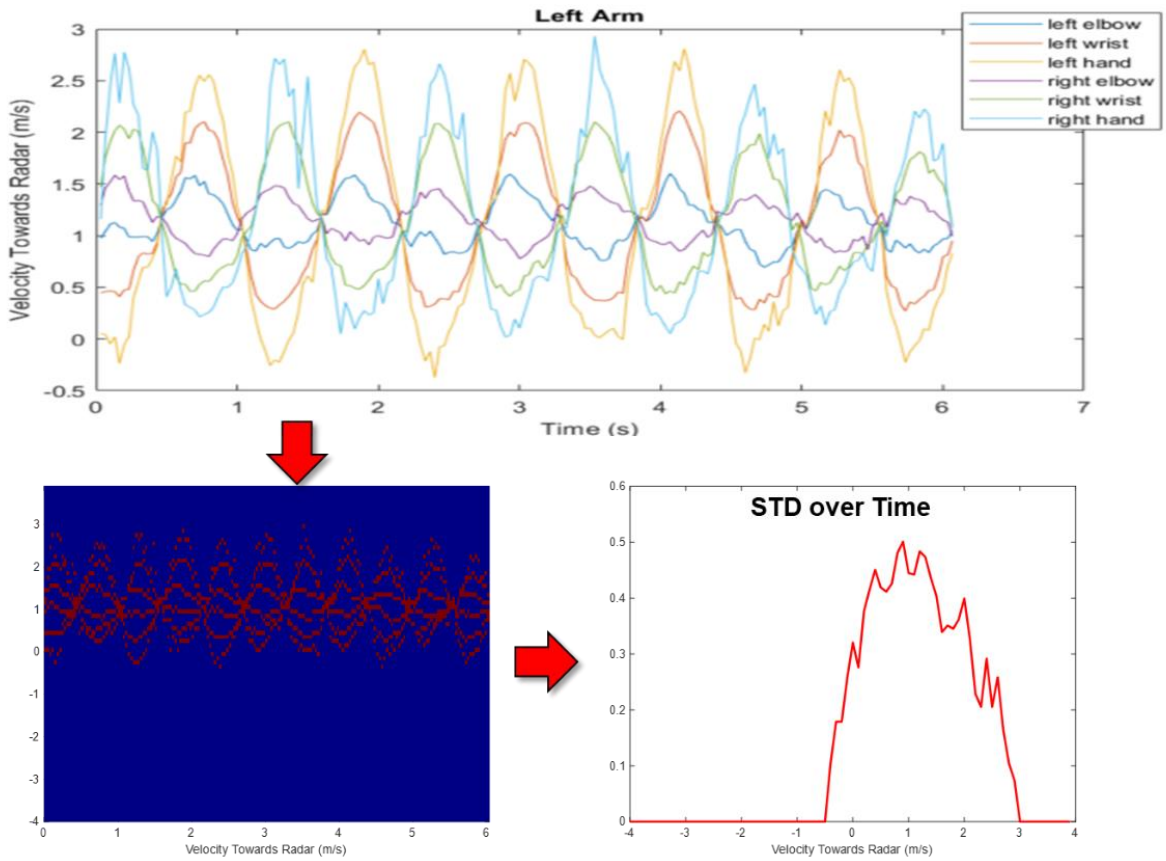

Figure 14 – Processed MD velocity STD data from actual motion captured data of arms and feet.

5 Bicycle Micro-Doppler Study

We also started the data collection and processing of bicyclist MD signatures. To help understanding the mechanisms of the MD signatures generation in bicyclist case, all moving parts such as both wheels, pedals, and rider will be added to measurements one by one.

Due to wintery weather conditions in central Ohio, the team is currently conducting radar measurements indoors. Figure 15 shows the OSU-ESL Indoor 77 GHz radar measurement setup for studying bicyclist MD responses. From left to right, the pictures show bike only, bicyclist in 0º, 30º, 60º, and 90º orientations. The mountain bike was mounted firmly on stands cover with microwave absorbing materials. The speeds of wheel and pedal rotations are monitored by sensors Table 1 summarizes currently completed bicyclist MD signature data collections. These testing scenarios include wheel rotation with and without pedaling, cyclists with and without additional movement, and the rotation of a detached wheel. From this data, the team can extrapolate relationships between wheel angles, velocities, and the presence of MD signatures. Additional testing scenarios are being developed to further classify cyclists from other VRUs by extracting and analyzing their unique micro-Doppler signatures.

Table 1 – Currently completed bicyclist MD signature data collections.

	Without human, wheels rotating	**Human pedaling on bicycle**
Location	Indoor	Indoor
Velocities (mph)	5~8 (slow), 15~17 (fast)	8~10 (slow), 19~21 (fast)
Angles (degree)	0, 30, 60, 90, 120, 180	0, 30, 60, 90
Distance (meters)	3~4	3~5

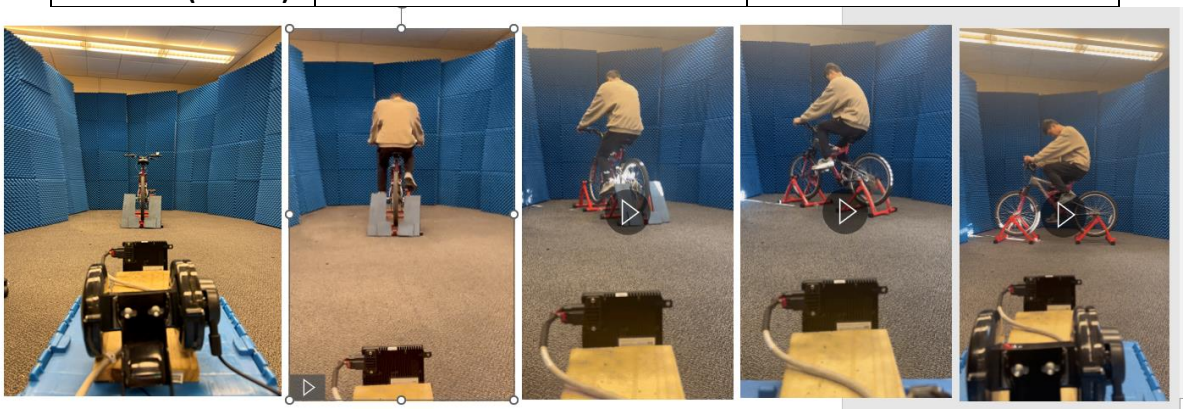

Figure 15 – OSU-ESL Indoor 77 GHz radar measurement setup for studying bicyclist MD responses.

Figure 16 compares the collected MD velocity data vs. time of bicyclist in different orientations with respect to radar. The wheel rotating speed is approximately at 20 mph. The presence of many horizontal lines in the top plot is typical for bike wheel due to scattering from many spokes. The second plot of the 30^{o} case shows some slower and stronger (more yellowish) responses which are likely produced by the pedaling legs. For the 90^{o} case, most of the horizontal lines almost disappears due to no distance changes from the spokes to radar. There are some lower velocity responses which could be caused by (1) relatively short radar distance, (2) knees' side movements during pedaling, and (3) scattering from the far side of leg which was blocked by the front legs periodically.

Figure 17 to Figure 20 shows the preliminary MD process results for one wheel turning at 8 mph and 20 mph without rider. These data were for 0^{o}, 30^{o}, 60^{o}, and 90^{o} bike orientations. It is observed that the MD signatures appear to be similar with or without a rider. This could be because of the zero-velocity filter placed in the processing code which would remove rider's strong body scattering in this indoor stationary setup. We will investigate this further by collecting some outdoor test data when weather permits.

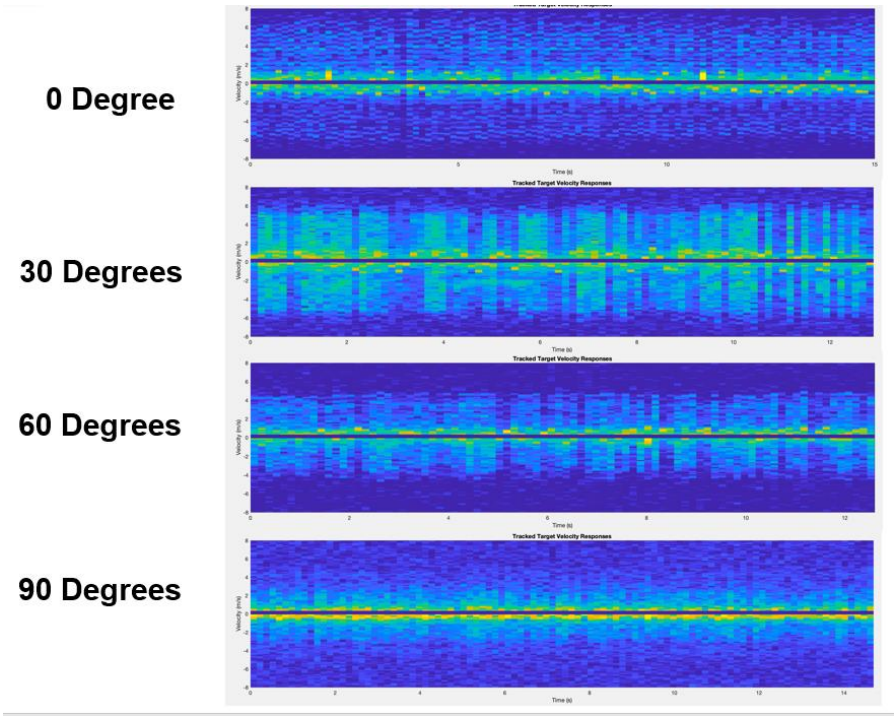

Figure 16 Collected MD velocity data vs. time of bicyclist in different orientations with respect to radar. The wheel rotating speed is approximately at 20 mph.

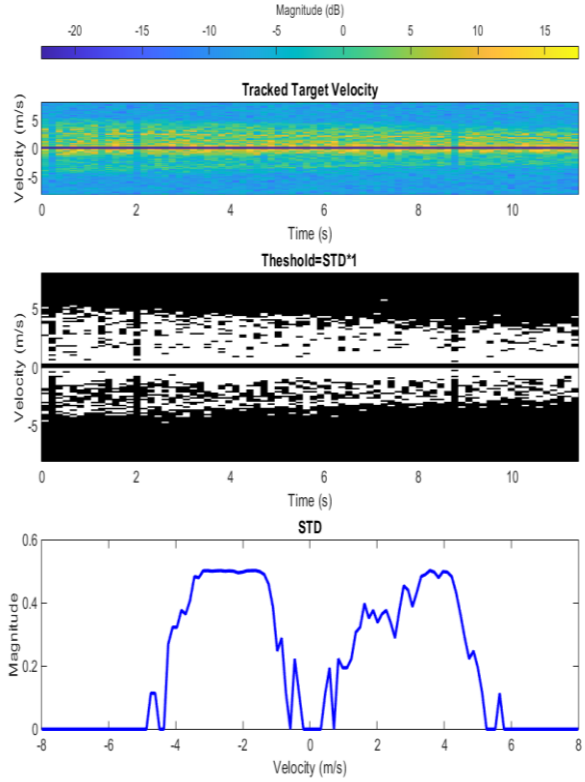

Figure 17 – Only wheel turning at 8 mph in 0°.

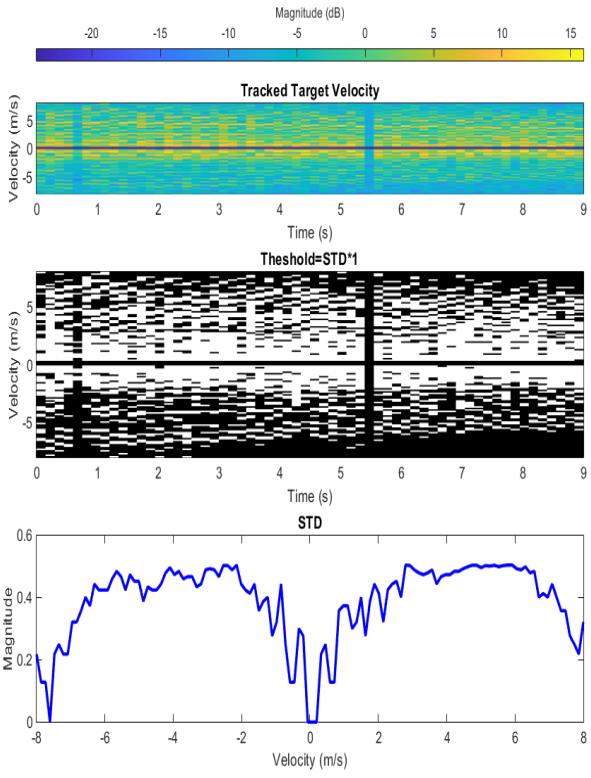

Figure 19 - Only wheel turning at 20 mph in 0°.

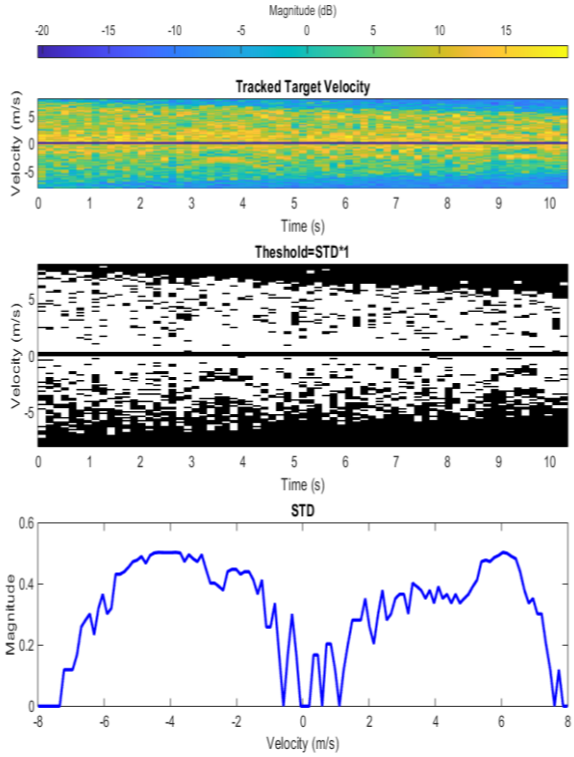

Figure 18 - Only wheel turning at 20 mph in 30°.

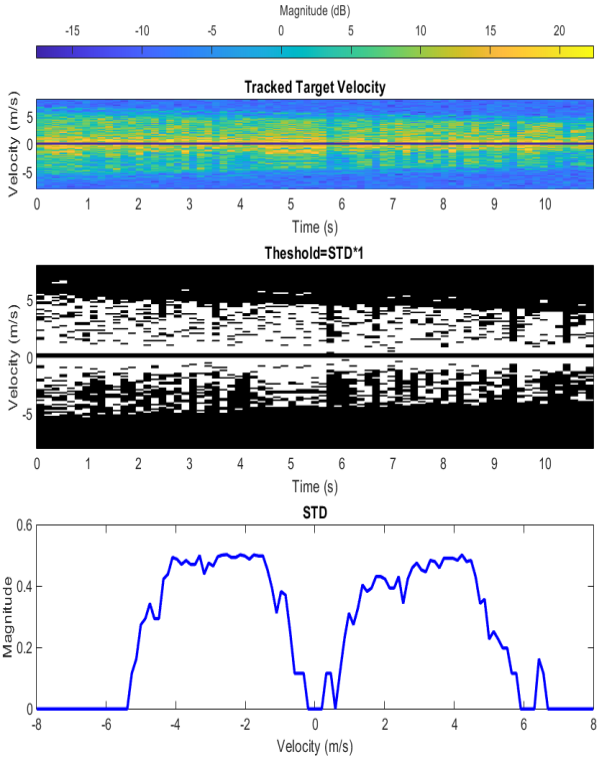

Figure 19 - Only wheel turning at 20 mph in 60°

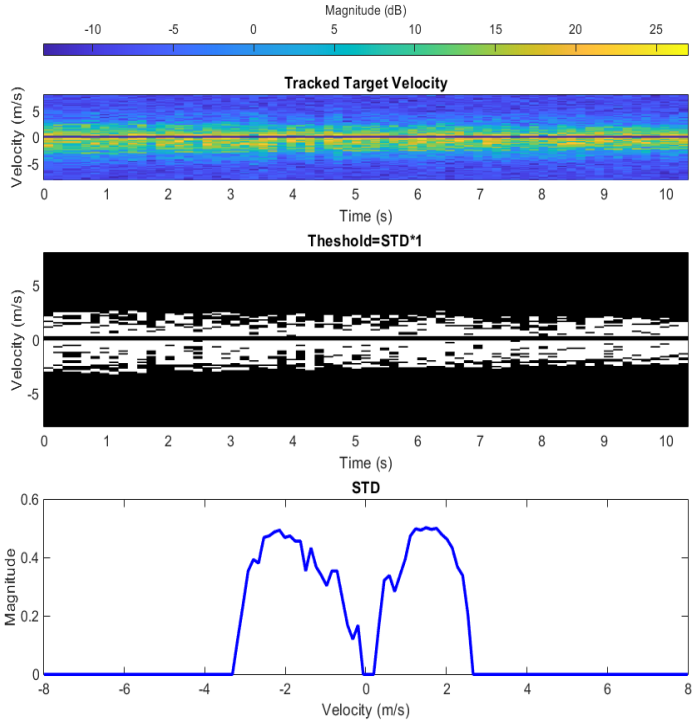

Figure 20 - Only wheel turning at 20 mph in 90°.

Figure 21 to Figure 26 show the preliminary MD processed reulsts for bicyclist rinding at 8 mph and 20 mph, in 0^{o}, 30^{o}, 60^{o}, and 90^{o} bike orientations.

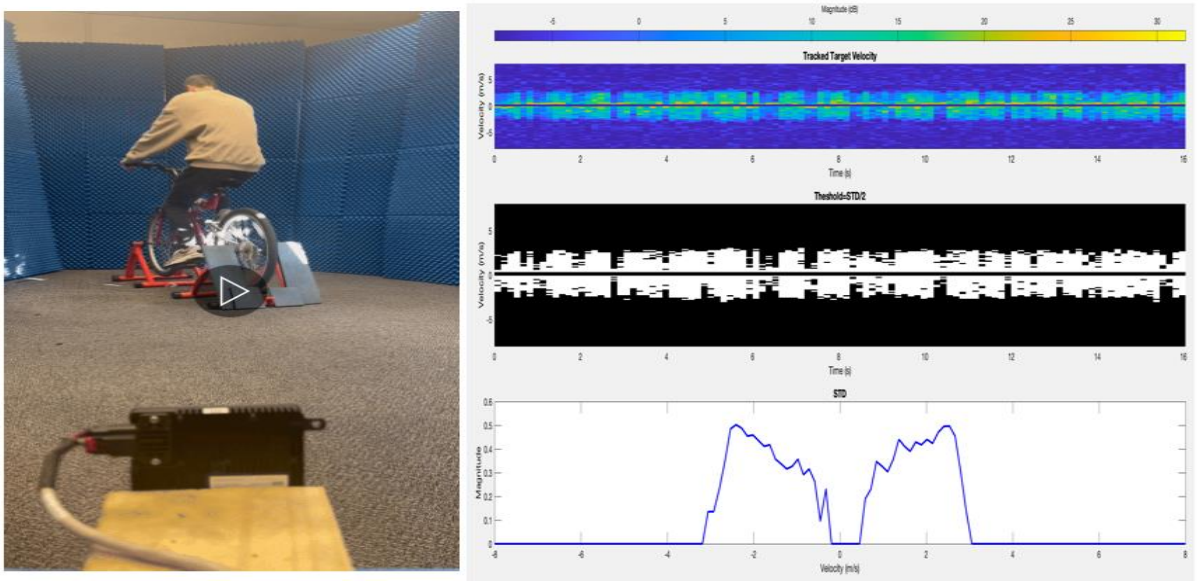

Figure 21 - Rider biking at 8 mph in 30^{o} orientation.

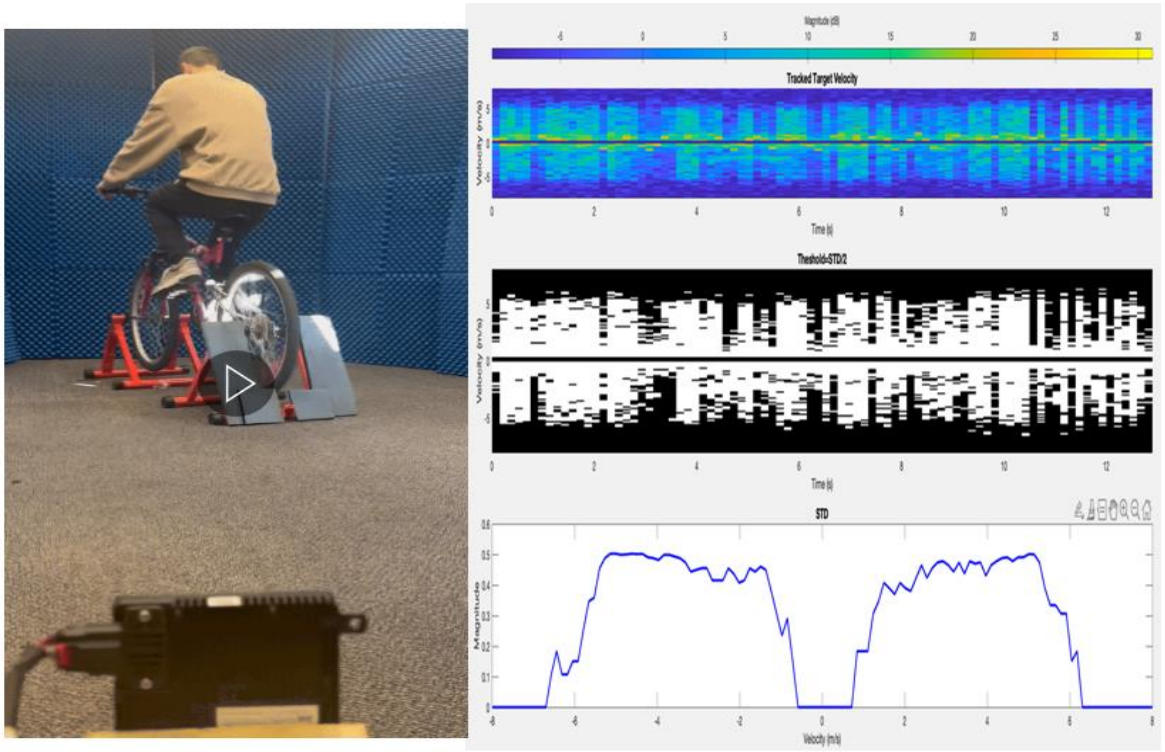

Figure 22 : Rider biking at 20 mph in 30^{o} orientation.

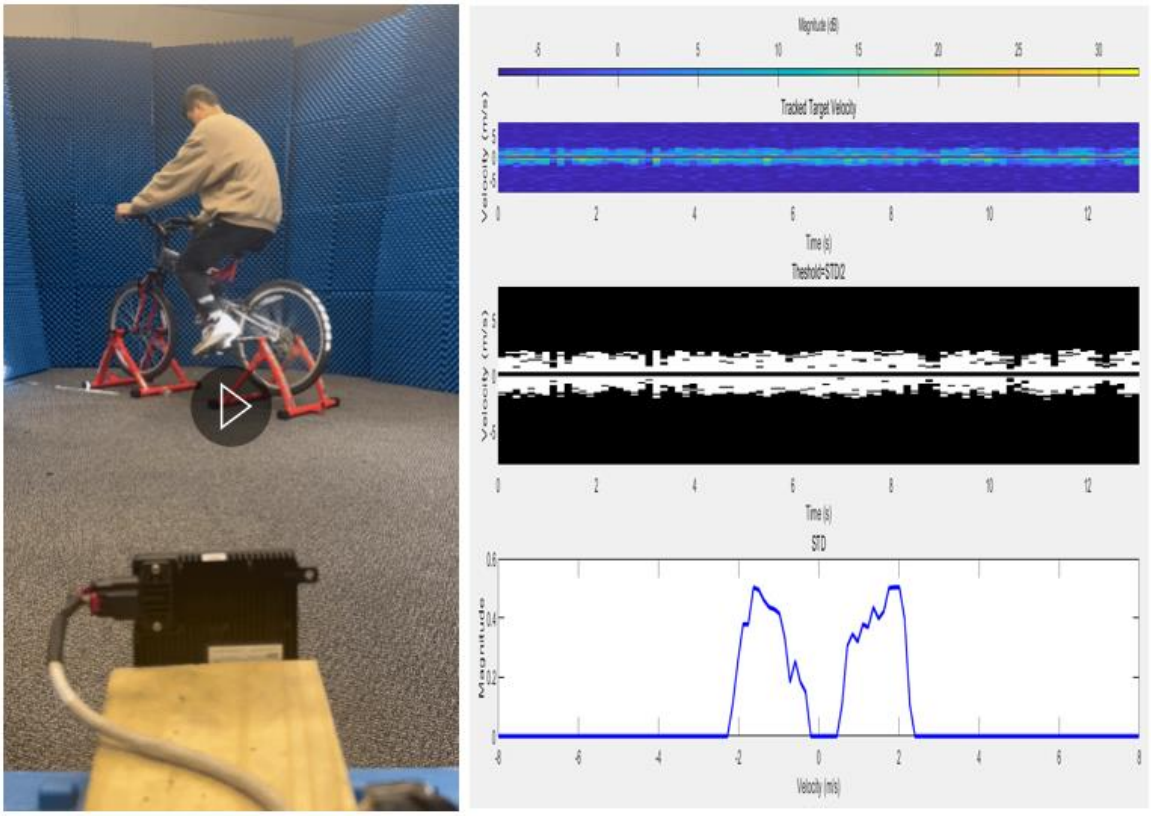

Figure 23 – Rider biking at 8 mph in 60^{o} orientation.

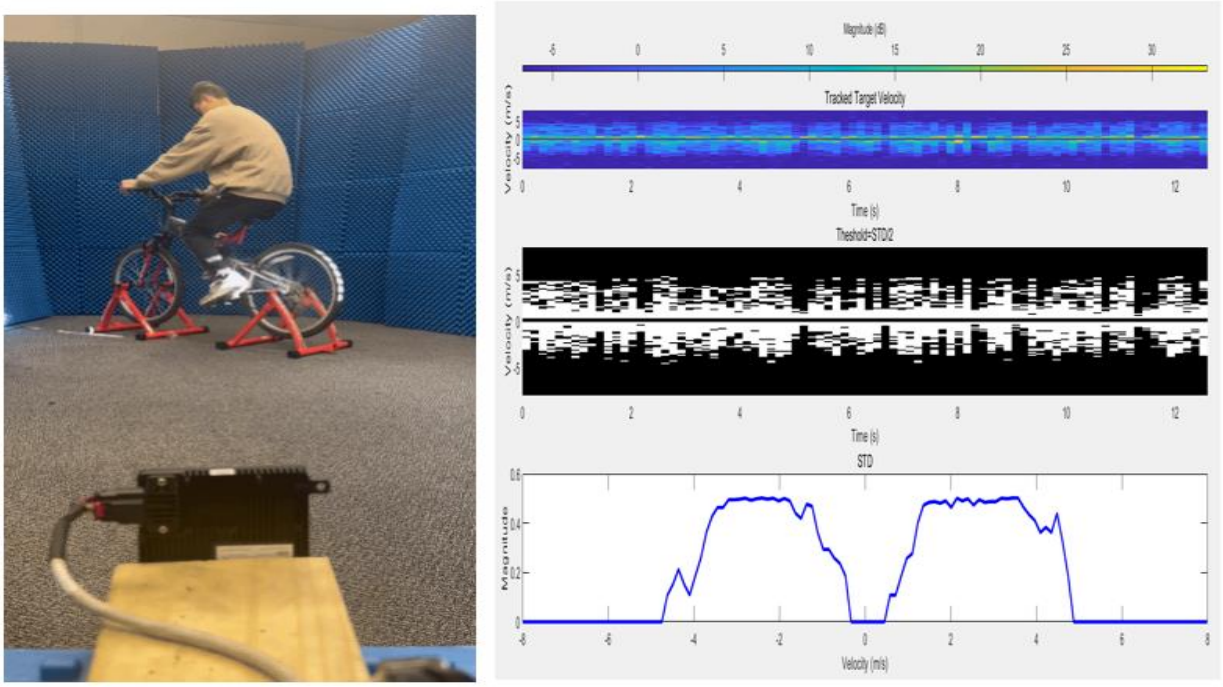

Figure 24 Rider biking at 20 mph in 60^{o} orientation.

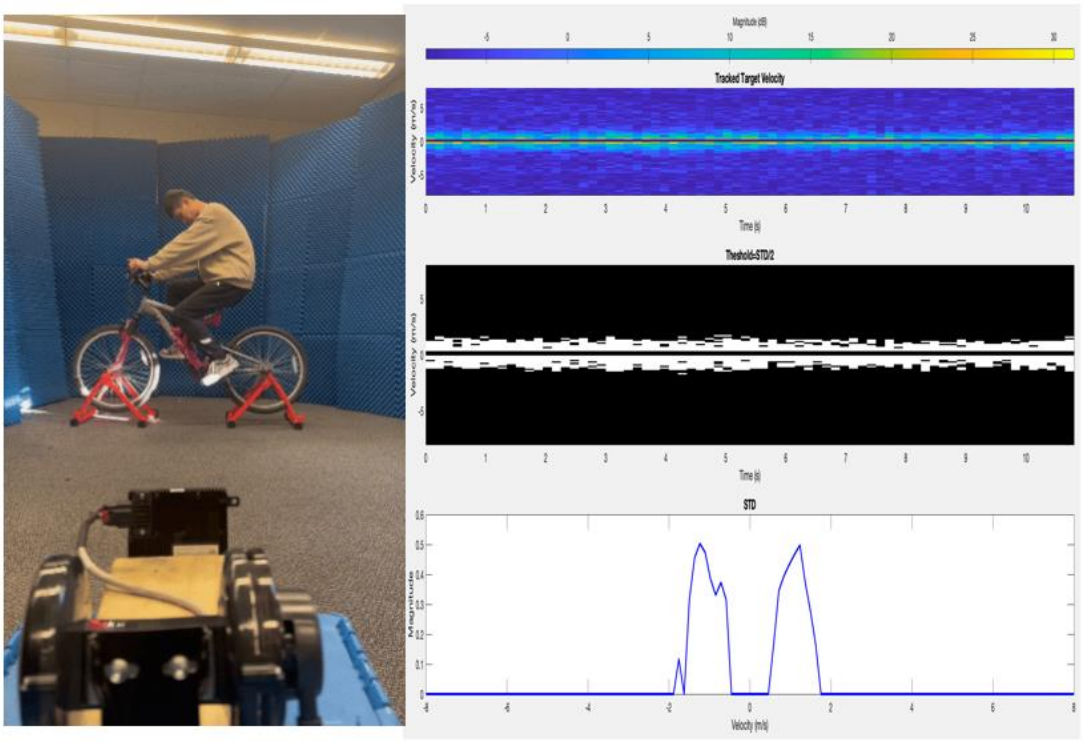

Figure 25 - Rider biking at 8 mph in 90° orientation.

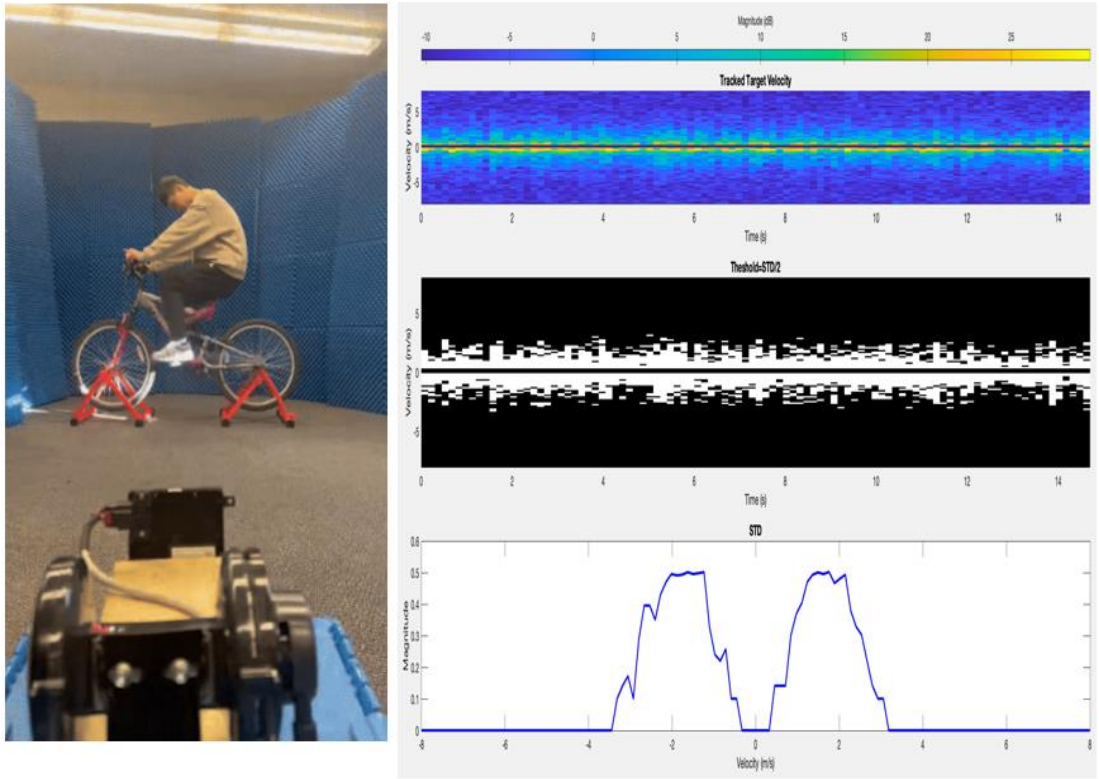

Figure 26 – Rider biking at 20 mph in 90° orientation.